Efficient, Near-Infrared Light-Induced Photoclick Reaction Enabled by Upconversion Nanoparticles

Fu, Y.; Wu, K.; Alachouzos, G.; Simeth, N.A.; Freese, T.; Falkowski, M.; Szymanski, W.; Zhang, H.; Feringa, B.L.

DOI
10.1002/adfm.202306531

Publication date
2023

Document Version
Final published version

Published in
Advanced Functional Materials

ADVANCED FUNCTIONAL MATERIALS
www.afm-journal.de

Efficient, Near-Infrared Light-Induced Photoclick Reaction Enabled by Upconversion Nanoparticles

Youxin Fu, Kefan Wu, Georgios Alachouzos, Nadja A. Simeth, Thomas Freese, Michal Falkowski, Wiktor Szymanski, Hong Zhang,* and Ben L. Feringa**

Photoclick reactions combine the selectivity of classical click chemistry with the high precision and spatiotemporal control afforded by light, finding diverse utility in surface customization, polymer conjugation, photocross-linking, protein labeling, and bioimaging. Nonetheless, UV light, pivotal in prevailing photoclick reactions, poses issues, especially in biological contexts, due to its limited tissue penetration and cell-toxic nature. Herein, a reliable and versatile strategy of activating the photoclick reactions of 9,10-phenanthrenequinones (PQs) with electron-rich alkenes (ERAs) with near infrared (NIR) light transduced by spectrally and structurally customized upconversion nanoparticles (UCNPs) is introduced. Under NIR irradiation, the UCNPs become UV/blue nanoemitters uniformly distributed in the reaction system. Enabled by the customized UCNPs, 800 or 980 nm light effectively activates the photocycloaddition reactions via radiative energy transfer in both general and triplet–triplet energy transfer (TTET)-mediated PQ-ERA systems. In particular, the novel sandwich structure UCNPs achieve the click reaction with up to 76% production yield in 10 min under NIR light irradiation. Meanwhile, the tricky side effect of photoclick product absorption-induced quenching is successfully circumvented from the fine-tuning of the upconversion spectrum. Moreover, through-tissue irradiation experiments, the authors show that the UCNP-PQ-ERA reaction unlocks the full potential of photoclick reactions for in vivo applications.

1. Introduction

Light-triggered cycloaddition reactions, also known as photoclick reactions,[1–3] combine the advantages of both photochemistry[4] and classical click chemistry[5–8] and thus, enable chemoselective product formation, quantitative conversion, short reaction times, high functional group orthogonality, and mild reaction conditions with the potential for superb spatiotemporal resolution. The last decade has witnessed the booming development of photoclick chemistry since the first report published in 2008 by Lin and coworkers.[9] The introduced reactions include photo-induced tetrazole-alkene cycloadditions,[10] UV-light initiated thiol-ene and thiol-yne reactions,[11] light-induced *o*-naphthoquinone methides (*o*NQMs)-ene hetero-Diels–Alder cycloaddition,[12] light-triggered azide-alkyne cycloadditions,[13] photo-induced sydnone-alkene/alkyne cycloadditions,[14] photo-induced azirine-alkene cycloaddition,[15] light-triggered oxime ligation reactions,[16] light-mediated coupling of acylsilanes with indoles,[17] and visible-light-induced 9,10-phenanthrenequinone-electron-rich alkene (**PQ-ERA**) photocycloadditions.[18–21] Collectively, these photoclick reaction systems have rapidly become indispensable as a methodology for surface functionalization,[12,22,23] polymer conjugation,[24,25] photocross-linking,[26] protein labeling,[27–29] and bioimaging.[18,20,30]

To date, most of these classical photoclick reactions require UV light irradiation, which renders them unsuitable for biological

Y. Fu, G. Alachouzos, N. A. Simeth, T. Freese, M. Falkowski, W. Szymanski, B. L. Feringa
Centre for Systems Chemistry
Stratingh Institute for Chemistry
Faculty for Science and Engineering
University of Groningen
Nijenborgh 4, 9747 AG Groningen, The Netherlands
E-mail: w.szymanski@umcg.nl; b.l.feringa@rug.nl

The ORCID identification number(s) for the author(s) of this article can be found under https://doi.org/10.1002/adfm.202306531

DOI: 10.1002/adfm.202306531

K. Wu, H. Zhang
Van't Hoff Institute for Molecular Sciences
University of Amsterdam
Science Park 904, 1098 XH Amsterdam, The Netherlands
E-mail: h.zhang@uva.nl

N. A. Simeth
Institute for Organic and Biomolecular Chemistry
Georg-August-University Göttingen
Tammanstraße 2, 37077 Göttingen, Germany

W. Szymanski
Department of Radiology
Medical Imaging Center
University of Groningen
University Medical Centre Groningen
Hanzeplein 1, 9713 GZ Groningen, The Netherlands

applications, as UV light does not penetrate effectively through biological tissue and is toxic to cells.[1–3] Efficient photoclick reactions, induced by substantially lower energy photons (e.g., wavelengths in the red-shifted visible (λ = 450–760 nm) and even near-infrared (λ = 760–2500 nm) range), are thus pursued,[31,32] considering that this wavelength range satisfies the requirements of deep tissue penetration,[33] higher signal-to-noise ratio (lower tissue autofluorescence),[34] and low phototoxicity.[35] In addition, visible/NIR light sources are more common on the market and accessible to nonspecialist end-users than high-energy ultraviolet-light sources.[32]

To address the need for photoclick reactions activated with visible/NIR light, several strategies have been developed, such as extending the π-conjugation of photoclick reactants,[36,37] using triplet–triplet energy transfer (TTET),[38] two-photon excitation,[39,40] and upconversion nanoparticles (**UCNP**s).[41,42] Among them, directly shifting the absorption band of photoclick reactants by extending their π-conjugation complicates their synthesis, while redshifting the wavelength of irradiation via TTET, as we reported recently,[38] is limited to orange light (590 nm) so far and not yet sufficient to trigger deep-tissue photoreactions. Further decreasing the energy of light required to initiate the photoclick reaction could be realized via two-photon excitation technology reaching the NIR light, which shows good penetration ability.[43] However, two-photon absorption requires high-intensity pulsed laser light (pulse intensity $>10^6$ W cm^{-2}) and the process is usually inefficient.[44]

Lanthanide-doped **UCNP**s, due to their high chemical stability, narrow emission bandwidth, and long luminescence lifetime, can effectively convert continuous wave NIR light into UV or visible emission.[45,46] **UCNP**s can achieve highly effective luminescence and a wider upconverting band under more economical continuous wavelength (CW) laser.[47] Furthermore, nano-sized particles can be monodispersed in organic solvents and well mixed with organic compounds.[48] With **UCNP**s transducers, NIR light can trigger photoreactions, including photolysis,[49] photoisomerization,[50–52] photocycloaddition,[41,42] and photopolymerization.[53] For instance, they have enabled the two-way photoswitching of dithienylethene,[54] the reversible control over the reflection of liquid crystals,[55–57] and the modulation of the biocatalytic activity of bacteria.[58] Recently, Barner-Kowollik and coworkers demonstrated that nitrile imine-mediated tetrazole-ene cycloadditions (**NITEC**) can be activated with 974 nm NIR light by **UCNP** addition.[41] However, the using of pure MeCN as a solvent, high power (14 W) of laser, and long irradiation time necessary to reach full conversion (over 40 min) may limit its further application. Thus, developing efficient, fast, and low power NIR light-driven photoclick reaction remains challenging.

Among all photoclick reactions, the 9,10-phenanthrenequinone (**PQ**)–electron-rich alkene (**ERA**) photocycloadditions have garnered significant interest due to its favorable kinetics, biocompatibility, responsiveness to visible light, high photoreaction quantum yield, and also the remarkable fluorescence properties exhibited by the photoclick products. Our recent findings have demonstrated its potential for advancing chemical biology and medical imaging.[18] Nonetheless, it is noteworthy that the current limitations of this reaction lie in its restricted activation wavelengths confined to the blue and green light region.[18–21] Unfortunately, light within this range possesses inadequate tissue penetration capabilities, thereby constraining the in vivo applications, emphasizing the importance to use NIR light. To tackle the main challenge identified, we introduce for the first time a reliable and versatile strategy to NIR light-induced **PQ-ERA** photoclick reactions using **UCNP** (**Scheme 1**). Taking advantage of the excellent overlap of **PQ**s or photosensitizer absorption spectra, respectively, and **UCNP**s emission spectra, the emitted light from **UCNP**s (excitation by NIR light) could be efficiently reabsorbed by the **PQ**s or photosensitizer systems. This results in the efficient photocycloaddition reactions in both general **PQ-ERA** (Scheme 1C) and TTET-induced **PQ-ERA** (Scheme 1D). Furthermore, as a proof of principle experiment, we demonstrate the potential of **UCNP-PQ-ERA** system for its application in vivo by showing deep tissue penetration through a chicken muscle.

2. Results and Discussion

The synthesis of the **UCNP**s and the **PQ** derivatives were described previously (for detailed information, see Section S2, Supporting Information).[21,38,46,59,60] For the NIR light-induced **PQ-ERA** photoclick reaction to proceed efficiently, sufficient spectral overlap between the emission of **UCNP**s, and the absorption spectrum of the **PQ**s or the TTET-promoting photosensitizer, respectively, must be ensured. To satisfy this design requirement under different reaction conditions, four **UCNP**s were employed in this study, namely $NaYF_4$@$NaYF_4$:75%Yb^{3+}, 0.5%Tm^{3+}@$NaYF_4$ (**UCNP 1**, sandwich core–shell–shell, Figure S25, Supporting Information),[61] $NaYF_4$:80% Yb^{3+}, 2% Er^{3+}@$NaYF_4$ (**UCNP 2**, core–shell, Figure S26, Supporting Information),[62] $NaYF_4$:40%Yb^{3+}, 2%Er^{3+}@$NaYF_4$ (**UCNP 3**, core–shell, Figure S27, Supporting Information),[62] and $NaYF_4$:40% Yb^{3+}, 2% Er^{3+}@$NaYbF_4$@ $NaYF_4$:30% Nd^{3+} (**UCNP 4**, core–shell–shell, Figure S28, Supporting Information).[61,63] From the transmission electron microscopy (TEM) images, and X-ray diffraction results (**Figure 1**A,B; for detailed information, see Section S4.2 and Figures S40–S45, Supporting Information), hexagonal-phased nanoparticles **UCNP 1–4** were obtained as monodisperse, with a uniform size, which demonstrates the homogeneity of the **UCNP** samples.

We next screened the **UCNP**s regarding compatibility of their luminescence properties with the **PQ-ERA** system (Figures 1C and 4B; Figure S31, Supporting Information), showing excellent spectral overlap of the upconversion emission and the absorptions of **PQ**s or the photosensitizer (**DiIbodipy**), respectively. In the region of 330–420 nm, **UCNP 1** (codoped Yb $^{3+}$ and Tm^{3+}) emitting at 340 and 360 nm ($^1I_6 \rightarrow {}^3F_4$, $^1D_2 \rightarrow {}^3H_6$, Figure S25 and for detailed information, see Section S4.1, Supporting Information) and **UCNP 2** and **3** (codoped Yb $^{3+}$ and Er $^{3+}$) emitting at 380 and 408 nm ($^2H_{9/2} \rightarrow {}^4I_{15/2}$, Figures S26–S27 and for detailed information, see Section S4.1, Supporting Information), overlap well with the absorption spectrum of **PQ-3TP**, **PQ-3DiTP**, and **PQ-3Furan** (Figure 1C and Figure S32, Supporting Information). In the region 510–550 nm, **UCNP 2–4** emit at 520 and 540 nm ($^2H_{11/2} \rightarrow {}^4I_{15/2}$, $^4S_{3/2} \rightarrow {}^4I_{15/2}$, Figures S26–S28 and for detailed information, see Section S4.1, Supporting Information), and thus match well with the absorption spectrum of **DiIbodipy** (Figure 4B). Performing quenching experiments, we additionally

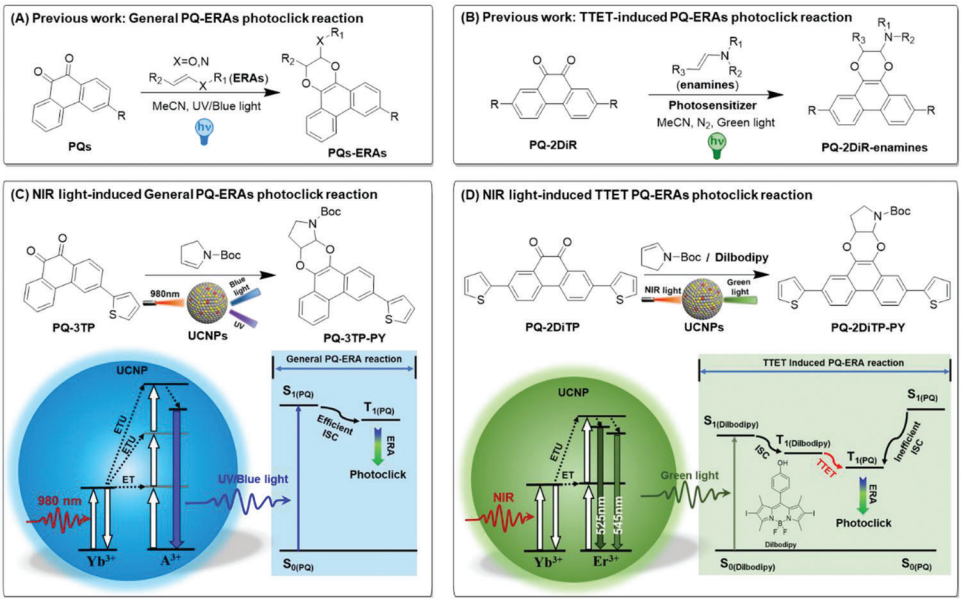

Scheme 1. Schematic illustration of photocycloaddition of 9,10-phenanthrenequinone **(PQ)** with electron-rich alkenes (**ERA**s). The state-of-the-art: A) UV/Blue light-triggered general **PQ-ERA** photoclick reaction and B) green light-induced TTET **PQ-ERA** photoclick reaction. The novel NIR light-induced **PQ-ERA** photoclick reaction presented here with: C) general and D) TTET system assisted by **UCNP**s addition. For C) and D), all energy levels are simplified, A^{3+} refer to Er^{3+} or Tm^{3+}.

found that the upconverting emission intensity of the **UCNP**s greatly decreases with an increasing concentration of **PQ**s and **DiIbodipy** (Figures S33–S39 and for detailed information, see Section S4.1, Supporting Information). We can thus conclude that the upconversion emission is effectively absorbed by **PQ**s and **DiIbodipy** and the systems indeed have the potential to achieve NIR light-triggered direct and TTET-induced **PQ-ERA** photoclick reactions (Scheme 1C,D).

Then, one of the best performing **PQ-ERA** photoclick reactions, which involves **PQ-3TP** and *N*-boc-2,3-dihydro-1*H*-pyrrole (**PY**),[60] was chosen as model system (for a general reaction scheme, see Scheme 1A and Figure S47, Supporting Information) to test the hypothesis of a NIR light-induced **PQ-ERA** photoclick reaction, and to quantify the efficiency of the reaction compared with our established photoligations via **PQ-ERA**.[18,21,38,60] Furthermore, **PQ-3TP** exhibits remarkable stability even under the thermal effects induced by prolonged exposure to a high-intensity 980 nm laser (Section S4.3 and Figure S50, Supporting Information).

Next, **PQ-3TP** and **PY** were combined in MeCN under N_2 atmosphere in the presence of **UCNP 1**(1.5 mg mL^{-1}). The photoclick reaction progress was studied with UV–Vis spectroscopy (Figure 1D). The initially yellow colored solution exhibited an absorption maximum at ≈390 nm. Upon 980 nm (28 W cm^{-2}) NIR laser irradiation, the solution color changed gradually from yellow to colorless. Accordingly, there was a gradual reduction in the intensity of the absorption band at 390 nm while a new absorption band in the UV region of the spectrum was formed showing a λ_{max} around 334 nm (Figure S51B, Supporting Information). The observed behavior was analogous to that of the general **PQ-3TP+PY** photoclick reaction proceeding without the addition of **UCNP**s addition and irradiation with 390 nm UV light (Figure S47, Supporting Information). The formation of the [4+2] photocycloaddition product was also confirmed by UPLC-MS. The complete conversion of **PQ-3TP** was reached within 10 min using 980 nm laser irradiation, making this **UCNP-PQ-ERA** system competitive with the fastest photoclick reactions triggered by NIR light (Figure 1E, red line) known so far.[41,42] Next, we quantified the reaction process by HPLC analysis (Figures S69–S71 and for detailed information, see Section S4.4, Supporting Information). Our measurements showed a yield of 76% for the desired product and only minimal formation of side products in the crude NIR-irradiated reaction mixture (Figure S83B, Supporting Information). Besides, conventional core–shell **UCNP 1′** structure exhibited lower efficiency in the **PQ-ERA** photoclick reaction than that of the original sandwiched structure (Section S4.3 and Figures S52–S53, Supporting Information). Finally, to study the influence of possible thermal effects on the reaction, photothermal effect of highly Yb^{3+} or Nd^{3+} doped **UCNP** reaction systems was investigated. Under 980 nm irradiation, **UCNP 1** solution experienced an initial increase of 3 °C within a few seconds, followed by a rise of 3 °C over 2 h (Figure S46, Supporting Information, red line). In contrast, under 800 nm irradiation, the **UCNP 4** solution exhibited negligible photothermal effect, i.e., less than 1 °C within 2 h (Figure S46, Supporting Information, blue line). The results highlight the superior heat control achieved by utilizing the 800 nm irradiation, while the temperature change under 980 nm irradiation is acceptable.

Encouraged by these results, we continued to study the same NIR light-induced photoclick system containing **PQ-3TP+PY+UCNP 1** at lower laser power density (16 and 8 W cm^{-2}) to pave the way toward in vivo applications. At the lower laser intensities, a similar trend was also observed, albeit longer irradiation times were required to reach full conversion (25 and 70 min, respectively, Figure 1E). HPLC analysis showed that the reaction yields were decreased to 64% and 43% for 16 and 8 W cm^{-2},

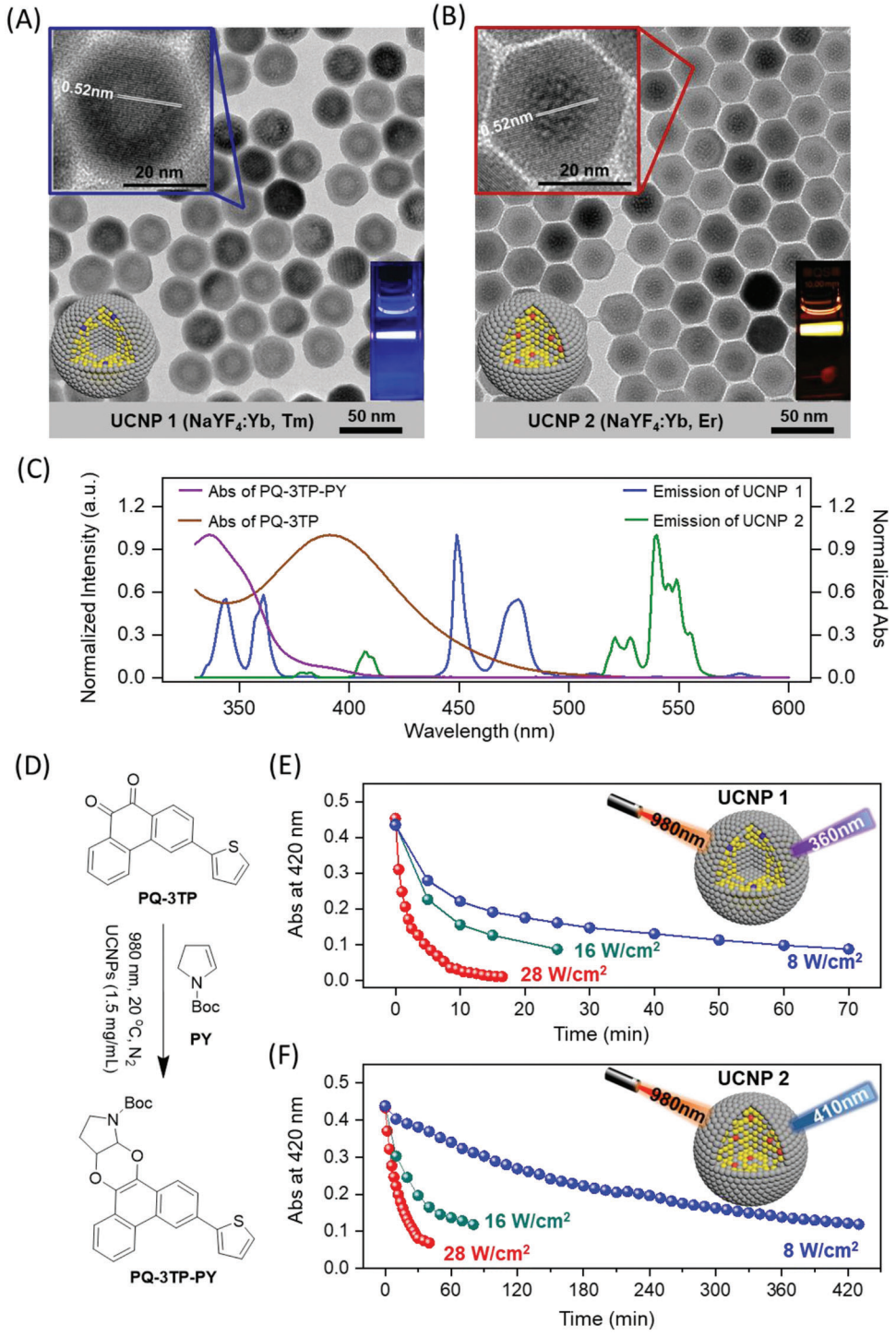

Figure 1. Overview of NIR light-induced PQ-3TP+PY photocycloadditions. Transmission electron microscopy (TEM) image of: A) **UCNP 1** and, B) **UCNP 2**. C) Overlap of the emission spectra of **UCNP**s (range: 325–600 nm, blue and green for **UCNP 1** and **UCNP 2**, respectively) and absorption spectra of **PQ-3TP** and **PQ-3TP-PY**. D) Reaction scheme of **PQ-3TP**+**PY** with **UCNP**s addition upon 980 nm laser irradiation. E,F) Kinetic traces (at 420 nm) of the photocycloaddition between **PQ-3TP** (50 μM) and **PY** (500 μM) with 1.5 mg mL^{-1} **UCNP**s (**UCNP 1** and **UCNP 2**, respectively) addition in 2.5 mL MeCN under N_2 atmosphere. The reaction mixture was irradiated with 980 nm laser (28, 16, 8 W cm^{-2}) at 20 °C and followed by UV–Vis absorption spectroscopy.

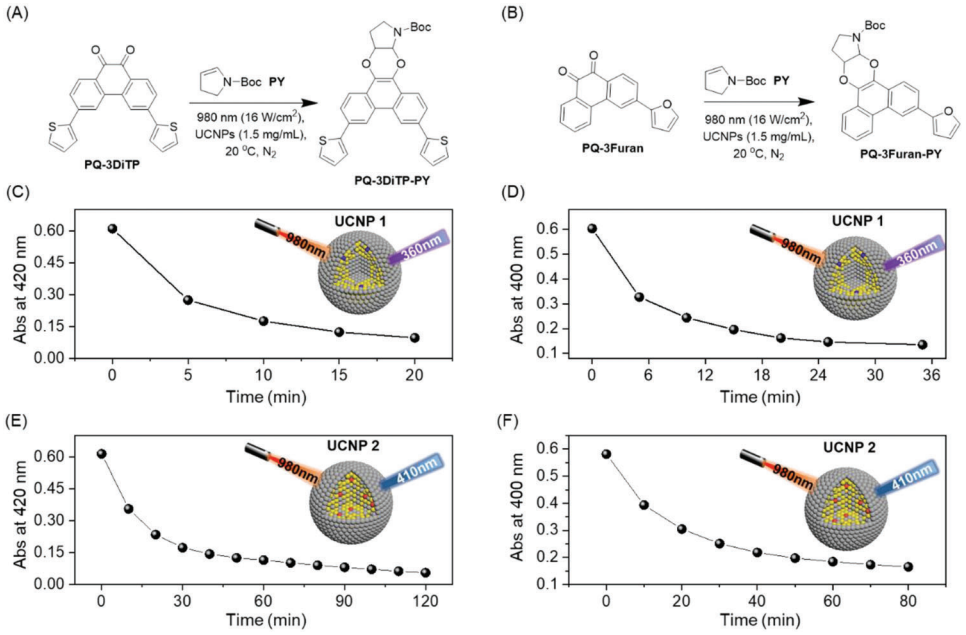

Figure 2. Substrate screening of NIR light-induced PQ-ERA photocycloadditions. Reaction scheme of: A) **PQ-3DiTP**+**PY** and B) **PQ-3Furan**+**PY** with **UCNP**s addition upon 980 nm laser irradiation. C,E) Kinetic traces (recorded at 420 nm) of the photocycloaddition between **PQ-3DiTP** (50 μM) and **PY** (500 μM) with 1.5 mg mL^{-1} **UCNP**s (**UCNP 1** and **UCNP 2**, respectively) addition in 2.5 mL MeCN with N_2 atmosphere. D,F) Kinetic traces (recorded at 400 nm) of the photocycloaddition between **PQ-3Furan** (50 μM) and **PY** (500 μM) with 1.5 mg mL^{-1} **UCNP**s (**UCNP 1** and **UCNP 2**, respectively) addition in 2.5 mL MeCN with a N_2 atmosphere. The reaction mixture was irradiated with 980 nm laser (16 W cm^{-2}) at 20 °C and followed by UV–Vis absorption spectroscopy.

respectively (Figures S72–S73 and S83B, Supporting Information). The lower yields could be ascribed to a decomposition product that was observed in **PQ-3TP+PY+UCNP 1** system at prolonged irradiation times with the 980 nm laser. These findings can be rationalized by a significant overlap between the **UCNP 1** emission band and the absorption band of the desired **PQ-3TP-PY** photoclick product (Figure 1C).

To alleviate the photodegradation concern, we redshifted the upconversion emission to 380 and 408 nm with core–shell structure **UCNP 2**, which corresponds to the transition $^2H_{9/2} \rightarrow {}^4I_{15/2}$ of Er^{3+} under 980 nm excitation (Figure S26, Supporting Information). The spectral overlap with the energetically lowest absorption of **PQ-3TP** is satisfying (Figure 1C). More importantly, the spectral overlap with the photoclick product **PQ-3TP-PY** can be avoided, which may circumvent photodegradation of the product (Figure 1C). To explore this, we repeated the same photoclick experiment as described above, now using **UCNP 2** as the upconverting system. We monitored the reaction by UV–Vis absorption spectroscopy (Figure S54 and Section S4.3, Supporting Information), and observed a similar change in the absorption spectrum upon 980 nm light irradiation as in the **UCNP 1** system (Figure 1F). The formation of the desired photoclick reaction product was confirmed with HPLC and yields of 68%, 50%, and 49% were obtained depending on the laser intensity (for 28, 16, and 8 W cm^{-2}, respectively; Figures S74–S76 and S83B, Supporting Information). Strikingly, no photodegradation was observed during this process, even with persistent 980 nm laser irradiation (Figure S48, Supporting Information). Meanwhile, the corresponding control experiment in the absence of **UCNP**s did not yield any of the desired photoclick cycloadduct (Figure S49 and for detailed information, see Section S4.3, Supporting Information). In addition, we examined the effectiveness of a sandwich structure using Er^{3+} doped **UCNP 2′** ($NaYF_4$@$NaYF_4$:80%Yb^{3+}, 2% Er^{3+}@$NaYF^4$) in the NIR light-induced **PQ-ERA** photoclick reaction as a control. Results obtained are similar to that of the original core–shell structure **UCNP 2** (Section S4.3 and Figure S55, Supporting Information).

After achieving the successful photoinduced coupling chemistry for **PQ-3TP+PY** in the NIR-triggered upconversion system, we turned our attention to two further **PQ** derivatives, namely **PQ-3DiTP** and **PQ-Furan**. We investigated their propensity to react with **PY** analogous to **PQ-3TP** in the presence of **UCNP 1** or **UCNP 2** to demonstrate the generalizability of our NIR light-induced **PQ-ERA** photoclick strategy (Figures S57–S60 and Section S4.3, Supporting Information). Gratifyingly, both compounds should a similar behavior as **PQ-3TP** forming the respective photocycloaddition products, **PQ-3DiTP+PY** and **PQ-3Furan+PY** (**Figure 2**), which was also confirmed by HPLC analysis (Figures S77–S79 and Section S4.4, Supporting Information). Control experiments showed that the same products are obtained in the absence of **UCNP**s under 390 nm irradiation (Figures S48–S49, Supporting Information); however, no product formation was observed under NIR laser irradiation. The results demonstrated that our **UCNP**s-assisted NIR light-induced **PQ-ERA** photoclick strategy is generally applicable and efficiently mediation **PQ-ERA** photoclick reactions.

Next, we explored to the deep-tissue penetration propensity of our NIR light-induced **PQ-ERA** photoclick reaction system (**Figure 3**A). **PQ-3TP** (50 μM, 1 eq), **PY** (500 μM, 10 eq), and **UCNP 2** (1.5 mg mL^{-1}) were combined in a cuvette (MeCN,

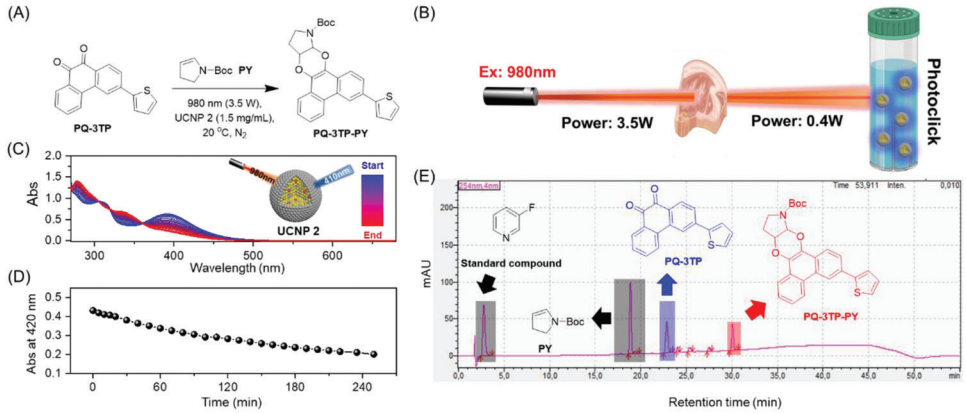

Figure 3. Overview of the penetration ability of NIR light-induced PQ-ERAs photoclick reaction. A) Reaction scheme and B) schematic illustration of the tissue penetration experiment setup: a 2-mm slice of a chicken breast muscle was placed between the beam and the reaction vessel to demonstrate the penetration capability of the near-infrared light. C) Time-resolved UV–Vis absorption spectra, D) kinetic traces (recorded at 420 nm), and E) HPLC analysis of the photocycloaddition between **PQ-3TP** (50 µM) and **PY** (500 µM) with **UCNP 2** (1.5 mg mL^{-1}) addition in 2.5 mL MeCN (N_2 atmosphere); the reaction mixture was irradiated with 980 nm laser (3.5 W) at 20 °C over 240 min.

N_2 atmosphere) covered with a 2-mm thick slice of chicken breast muscle (Figure 3B; Figure S4 and Section S1, Supporting Information). The sample was irradiated with 980 nm laser (3.5 W, 28 W cm^{-2}) and the process was monitored by UV–Vis absorption spectroscopy (Figure 3C,D). To our delight, the presence of the tissue did not much affect the [4+2] photocycloaddition product formation and the same trend was observed compared with the general **PQ-3TP+PY** photoclick reaction (**UCNP** 2 addition, 980 nm irradiation, Figure 1E) with longer irradiation time. Notably, the power intensity of the 980 nm laser was significantly attenuated after penetration through the chicken breast (a decay from 3.5 to 0.4 W was observed), which explains why prolonged irradiation times (>240 min) required to achieve a full conversion. Furthermore, mindful of the fact that the maximum permissible exposure of skin to NIR light within the wavelength range of 650–980 nm ranges from 0.2 to 0.726 W cm^{-2},[64] and aiming to further establish the potential value of this system in biological applications, we conducted additional penetration experiments (**PQ-3TP+PY+UCNP 2**) where the sample was covered by a 1 mm slice of chicken breast muscle. Low-intensity 980 nm NIR light (0.7 W cm^{-2}) was applied, and we closely monitored the changes in the UV–Vis absorption spectra. The results, depicted in Figure S61 (Supporting Information), clearly exhibit a discernible alteration in the UV–Vis absorption spectra as the irradiation time increased from 0 to 240 min. Remarkably, this change closely resembled the observations made in the previous high-intensity experimental group (Figure 3C) that confirms the generation of photoclick product, providing compelling evidence supporting their promising applications in biological systems.

While these results show that the photoclick reaction of **PQ**s bearing substituents in position 3 can be promoted with **UCNP**s and NIR light instead of direct irradiation with 390 nm light, we recently found that **PQ**s bearing electron-rich substituents in 2-position behave in a significantly different way: their direct activation with light leads to an inefficient intersystem crossing and very slow reaction.[38] However, the triplet state of **PQ** can be populated using a suitable photosensitizer, triggering the photoclick reaction via a TTET process. The additional benefit of this approach was that the wavelength of irradiation could be shifted to the green region (530 nm).

In addition, it is still worth noting that, in the Yb-Er upconversion system, as shown in Scheme 1D, the intensity of green emissions (520 and 540 nm) is much higher than blue emission (408 nm, Figures S26–S28, Supporting Information), which is caused by the upconversion quantum yield of blue emission (originating from three-photon excitation) being ten times lower than green emissions (originating from two-photon excitation).[65–67] However, it is difficult to harvest such high efficiency upconversion green light on the classical **PQ-ERA** photoclick reaction, since the poor overlap of the **UCNP 3** and **4** emission spectra and the 3-position substitution **PQ** absorption spectra.

Consequently, we were interested whether it would be possible to further bathochromically shift the photochemical stimulus by combining the TTET-sensitized **PQ-ERA** photoclick reaction system with upconversion nanoparticles. The chosen photosensitizer, **DiIBodipy**, exhibits a strong absorption around 520–530 nm range, which overlaps well with the emission spectrum of **UCNP 3** and **UCNP 4** (upon 980 and 800 nm laser excitation, respectively) and is thus promising to realize a **UCNP** assisted NIR light-induced, TTET-initiated **PQ-ERA** photoclick reaction (**Figure 4**A).

To verify this hypothesis, **DiIBodipy** (λ_{max} = 528 nm, Figure 4B) was employed as a photosensitizer for a TTET-initiated **PQ-ERA** photoclick reaction between **PQ-2DiTP** and **PY**. From previous TD-DFT calculations,[68–72] we know that the excited triplet T_1 state energy of **DiIBodipy** is 1.63 eV (for detailed information, see Section S5, Supporting Information) and hence slightly higher than the T_1 state energy of **PQ-2DiTP** (T_1 = 1.58 eV), suggesting that a TTET process from **DiIBodipy** to **PQ-2DiTP** can occur upon excitation of **DiIBodipy**. To test first the direct TTET process, **PQ-2DiTP**, **PY**, and **DiIBodipy** were combined in a cuvette (MeCN, N_2 atmosphere) and irradiated with 530 nm LED, where **DiIBodipy** (λ_{max} = 525 nm, Figure 4B) features a strong absorption. Progress of the reaction was

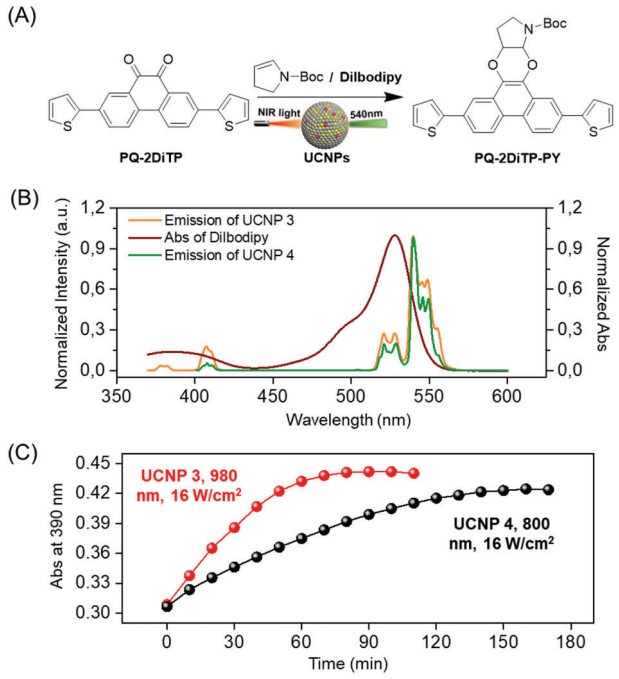

Figure 4. Overview of the NIR light-induced TTET-PQ-ERA photoclick reaction system. A) Schematic illustration of the NIR light-induced TTET-**PQ-ERA** photoclick reaction. B) Overlap of the emission spectra of **UCNP**s (yellow and green for **UCNP 3** and **UCNP 4**, respectively) and absorption spectra of photosensitizer-**DiIbodipy**. C) Kinetic traces (at 390 nm) of the photocycloaddition between **PQ-2DiTP** (50 μM) and **PY** (500 μM) with **DiIbodipy** (25 μM) and 1.5 mg mL^{-1} **UCNP**s (red line: **UCNP 3** and black line: **UCNP 4**, respectively) addition in 2.5 mL MeCN with N_2 atmosphere. The reaction mixtures were irradiated with 980 nm (**UCNP 3** group, 16 W cm^{-2}) and 800 nm (**UCNP 4** group, 16 W cm^{-2}) laser at 20 °C and followed by UV–Vis absorption spectroscopy.

monitored by UV–Vis absorption spectroscopy (for detailed information, see Section S4.2 and Figure S62, Supporting Information). An increase in the absorption band at 390 nm was observed, indicating the formation of [4+2] photoclick adducts, which was confirmed by UPLC-MS measurements. This enhancement reaches a plateau after ≈10 s (k_{obs}^{530}= 0.309 s^{-1}, Figure S62, Supporting Information), exhibiting a faster TTET-induced **PQ-ERA** photoclick reaction than our previously reported system.[38] Notably, this system also works efficiently in the presence of only 0.5% and 0.25% of **DiIBodipy** (k_{obs}^{530}= 0.0078 s^{-1} and 0.0043 s^{-1} respectively, Figure S63, Supporting Information).

Encouraged by these results, we then sought to explore the same TTET photoclick system using NIR light and **UNCP**s. We combined **PQ-2DiTP**, **PY**, **DiIBodipy**, and **UCNP 3** in a cuvette and irradiated with a 980-nm laser (28 and 16 W cm^{-2}), and we monitored the reaction by UV–Vis absorption spectroscopy (Figures S64–S65, Supporting Information). Confirming our hypotheses, upon 980 nm light irradiation, an increase in absorption band at 390 nm was observed and reached a plateau at 30 and 80 min using 28 and 16 W cm^{-2} intensity, respectively, (Figure 4C and Figure S56, Supporting Information). The formation of [4+2] photoclick adducts was confirmed by the HPLC analysis (Figures S68–S69 and Section S4.4, Supporting Information). Building on this, we conducted additional control experiments in the absence of a photosensitizer to confirm its importance (for detailed information, see Section S4.3 and Figures S66–S67, Supporting Information). The results unequivocally demonstrate that neither the utilization of a 530-nm LED (after 10 min of irradiation, Figure S66, Supporting Information) nor the application of a 980-nm laser (after 90 min of irradiation, Figure S67, Supporting Information) leads to the photoclick reaction in the absence of photosensitizers. This compelling evidence further emphasizes the pivotal significance of photosensitizers in the TTET-induced **PQ-ERA** photoclick system.

Finally, we also considered that the absorption of water and biological tissues around 980 remains non-negligible, which will attenuate the 980 nm excitation light and cause local heating at the irradiation site.[73] We thus employed **UCNP 4** which can be excited at 800 nm, where tissue is hardly absorbing and would consequently cause less thermal effects and better penetration. Upon 800 nm NIR laser irradiation, we indeed observed a similar trend in **PQ-2DiTP** conversion as in the presence of **UCNP 3** (Figure 4C; Figure S65B, Supporting Information). The HPLC analysis confirmed that we obtained the correct photoclick product (Figure S82, Supporting Information). To validate the superiority of the **UCNP 3** and **UCNP 4** systems, we also included **UCNP 1** in the NIR light-driven TTET-**PQ-ERA** photoclick reaction. While the emission spectrum of **UCNP 1** does exhibit some overlap with the absorption spectrum of **DiIBodipy** at 360 and 480 nm, the degree of overlap is relatively low (Figure S68B, Supporting Information). As anticipated, the **UCNP 1**-TTET system proved to be highly inefficient, as indicated by the lack of significant changes even after 90 min of exposure to a 980-nm laser (16 W cm^2; for detailed information, see Section S4.3 and Figure S68, Supporting Information). These findings strongly indicate that **UCNP 3** and **UCNP 4**, with their superior overlap between emission and the absorption of **DiIBodipy**, are better suited for facilitating the TTET-induced photoclick reaction. These results demonstrate the robustness and flexibility of our **UCNP**-assisted NIR light-induced photoclick reaction and its potential for in vivo labeling.

3. Conclusion

In summary, we report the first reliable and versatile strategy toward NIR light-induced **PQ-ERA** photoclick reaction. Different from traditional photochemistry in which external light directly induces the reaction, the nanoparticles **UCNP**s dispersed in the solution played the role of UV/blue nanoemitters uniformly distributed in the reaction system under NIR light irradiation. These novel **UCNP**s with specially designed nanostructures and tunable spectra improve significantly the upconversion emission intensities and spectral overlap with **PQ** absorption. Promoted by these **UCNP**s, efficient photocycloaddition reactions were achieved under 800 or 980 nm NIR light irradiation using two methodologies involving both general **PQ-ERA** and TTET-induced **PQ-ERA** systems. The transformations could be completed within 10 min with production yield as high as 76%, exhibiting the fastest and efficient photoclick reaction triggered by NIR light. Precise spectral customization of **UCNP**s circumvented successfully photodegradation of the reaction system. It was confirmed from the spectroscopy that the **UCNP**s activation of the photoclick reaction follows radiative energy transfer

mechanism. Notably, the deep-tissue penetration experiment employing chicken tissue showed the potential of the strategy to promote in vivo **PQ-ERA** photoclick reactions. We envision that this mild, efficient, fast NIR light-induced **PQ-ERA** photoclick reaction is not limited to the chemistry shown here but can be used in a wide range of applications, such as polymer conjugation, photopatterning, and photochemical cross-linking. Studies toward these applications and further developments to explore the full potential of this photoclick reaction manifold are now underway in our laboratories.

Supporting Information

Supporting Information is available from the Wiley Online Library or from the author.

Acknowledgements

Y.F. and K.W. contributed equally to this work. The authors thank Renze Sneep (University of Groningen) for his help with the HRMS measurements. The authors gratefully acknowledge the generous financial support from the Horizon 2020 Framework Program (ERC Advanced Investigator grant No. 694345 to B.L.F.), the Ministry of Education, Culture and Science of the Netherlands (Gravitation Program No. 024.001.035 to B.L.F.), and the European Molecular Biology Organization (EMBO LTF-232-2020 Postdoctoral Fellowship to G.A.). This research was supported by NWO domain TTW and Stryker European Operations Ltd. NWO TTW perspective project MEDPHOT, EU H2020MSCA-RISE-2017 Action program, CANCER, under grant No. 777682. M.F. acknowledges the Polish National Agency for Academic Exchange for the Bekker programme No. PPN/BEK/2020/1/00357.

Conflict of Interest

The authors declare no conflict of interest.

Data Availability Statement

The data that support the findings of this study are available in the supplementary material of this article.

Keywords

near-infrared light, phenanthrenequinone, photochemistry, photoclick chemistry, upconversion nanoparticles

Received: July 21, 2023
Revised: August 24, 2023
Published online: September 6, 2023

[1] B. D. Fairbanks, L. J. Macdougall, S. Mavila, J. Sinha, B. E. Kirkpatrick, K. S. Anseth, C. N. Bowman, *Chem. Rev.* **2021**, *121*, 6915.
[2] G. S. Kumar, Q. Lin, *Chem. Rev.* **2021**, *121*, 6991.
[3] M. A. Tasdelen, Y. Yagci, *Angew. Chem., Int. Ed.* **2013**, *52*, 5930.
[4] M. Montalti, A. Credi, L. Prodi, M. T. Gandolfi, *Handbook of Photochemistry*, 3rd ed., CRC Press, Taylor & Francis, Boca Raton, **2006**.
[5] H. C. Kolb, M. G. Finn, K. B. Sharpless, *Angew. Chem., Int. Ed.* **2001**, *40*, 2004.
[6] V. V. Rostovtsev, L. G. Green, V. V. Fokin, K. B. Sharpless, *Angew. Chem., Int. Ed.* **2002**, *41*, 2596.
[7] C. W. Tornøe, C. Christensen, M. Meldal, *J. Org. Chem.* **2002**, *67*, 3057.
[8] N. J. Agard, J. A. Prescher, C. R. Bertozzi, *J. Am. Chem. Soc.* **2004**, *126*, 15046.
[9] W. Song, Y. Wang, J. Qu, M. M. Madden, Q. Lin, *Angew. Chem., Int. Ed.* **2008**, *47*, 2832.
[10] W. Song, Y. Wang, J. Qu, Q. Lin, *J. Am. Chem. Soc.* **2008**, *130*, 9654.
[11] C. E. Hoyle, C. N. Bowman, *Angew. Chem., Int. Ed.* **2010**, *49*, 1540.
[12] S. Arumugam, V. V. Popik, *J. Am. Chem. Soc.* **2011**, *133*, 15730.
[13] A. A. Poloukhtine, N. E. Mbua, M. A. Wolfert, G.-J. Boons, V. V. Popik, *J. Am. Chem. Soc.* **2009**, *131*, 15769.
[14] L. Zhang, X. Zhang, Z. Yao, S. Jiang, J. Deng, B. Li, Z. Yu, *J. Am. Chem. Soc.* **2018**, *140*, 7390.
[15] R. K. V. Lim, Q. Lin, *Chem. Commun.* **2010**, *46*, 7993.
[16] T. Pauloehrl, G. Delaittre, M. Bruns, M. Meißler, H. G. Börner, M. Bastmeyer, C. Barner-Kowollik, *Angew. Chem., Int. Ed.* **2012**, *51*, 9181.
[17] C. Stuckhardt, M. Wissing, A. Studer, *Angew. Chem., Int. Ed.* **2021**, *60*, 18605.
[18] Y. Fu, H. Helbert, N. A. Simeth, S. Crespi, G. B. Spoelstra, J. M. van Dijl, M. van Oosten, L. R. Nazario, D. van der Born, G. Luurtsema, W. Szymanski, P. H. Elsinga, B. L. Feringa, *J. Am. Chem. Soc.* **2021**, *143*, 10041.
[19] A. Schönberg, A. Mustafa, *Nature* **1944**, *153*, 195.
[20] J. Li, H. Kong, L. Huang, B. Cheng, K. Qin, M. Zheng, Z. Yan, Y. Zhang, *J. Am. Chem. Soc.* **2018**, *140*, 14542.
[21] Y. Fu, N. A. Simeth, R. Toyoda, R. Brilmayer, W. Szymanski, B. L. Feringa, *Angew. Chem., Int. Ed.* **2023**, *62*, e202218203.
[22] S. Arumugam, V. V. Popik, *J. Am. Chem. Soc.* **2012**, *134*, 8408.
[23] T. Pauloehrl, G. Delaittre, V. Winkler, A. Welle, M. Bruns, H. G. Börner, A. M. Greiner, M. Bastmeyer, C. Barner-Kowollik, *Angew. Chem., Int. Ed.* **2012**, *51*, 1071.
[24] W. Feng, L. Li, C. Yang, A. Welle, O. Trapp, P. A. Levkin, *Angew. Chem., Int. Ed.* **2015**, *54*, 8732.
[25] C. Heiler, S. Bastian, P. Lederhose, J. P. Blinco, E. Blasco, C. Barner-Kowollik, *Chem. Commun.* **2018**, *54*, 3476.
[26] V. X. Truong, J. Bachmann, A. Unterreiner, J. P. Blinco, C. Barner-Kowollik, *Angew. Chem., Int. Ed.* **2022**, *61*, e202113076.
[27] D. F. Earley, A. Guillou, S. Klingler, R. Fay, M. Gut, F. d'Orchymont, S. Behmaneshfar, L. Reichert, J. P. Holland, *JACS Au.* **2022**, *2*, 646.
[28] Z. Yu, Y. Pan, Z. Wang, J. Wang, Q. Lin, *Angew. Chem., Int. Ed.* **2012**, *51*, 10600.
[29] Q. Xiong, T. Zheng, X. Shen, B. Li, J. Fu, X. Zhao, C. Wang, Z. Yu, *Chem. Sci.* **2022**, *13*, 3571.
[30] C. Wang, H. Zhang, T. Zhang, X. Zou, H. Wang, J. E. Rosenberger, R. Vannam, W. S. Trout, J. B. Grimm, L. D. Lavis, C. Thorpe, X. Jia, Z. Li, J. M. Fox, *J. Am. Chem. Soc.* **2021**, *143*, 10793.
[31] W. Szymański, J. M. Beierle, H. A. V. Kistemaker, W. A. Velema, B. L. Feringa, *Chem. Rev.* **2013**, *113*, 6114.
[32] R. Weinstain, T. Slanina, D. Kand, P. Klán, *Chem. Rev.* **2020**, *120*, 13135.
[33] C. S. Miller, D. K. White, *Oral Surgery, Oral Med. Oral Pathol. Oral Radiol. Endodontol.* **1996**, *82*, 57.
[34] S. He, J. Song, J. Qu, Z. Cheng, *Chem. Soc. Rev.* **2018**, *47*, 4258.
[35] Z. Zhang, W. Wang, M. O'Hagan, J. Dai, J. Zhang, H. Tian, *Angew. Chem., Int. Ed.* **2022**, *61*, e202205758.
[36] P. An, Z. Yu, Q. Lin, *Org. Lett.* **2013**, *15*, 5496.
[37] P. Lederhose, K. N. R. Wüst, C. Barner-Kowollik, J. P. Blinco, *Chem. Commun.* **2016**, *52*, 5928.
[38] Y. Fu, G. Alachouzos, N. A. Simeth, M. Di Donato, M. F. Hilbers, W. J. Buma, W. Szymanski, B. L. Feringa, Unpublished.

[39] Z. Yu, T. Y. Ohulchanskyy, P. An, P. N. Prasad, Q. Lin, *J. Am. Chem. Soc.* **2013**, *135*, 16766.
[40] C. D. McNitt, H. Cheng, S. Ullrich, V. V. Popik, M. Bjerknes, *J. Am. Chem. Soc.* **2017**, *139*, 14029.
[41] P. Lederhose, Z. Chen, R. Müller, J. P. Blinco, S. Wu, C. Barner-Kowollik, *Angew. Chem., Int. Ed.* **2016**, *55*, 12195.
[42] Y. Wu, J. Zheng, D. Xing, T. Zhang, *Nanoscale* **2020**, *12*, 10361.
[43] P. T. C. So, C. Y. Dong, B. R. Masters, K. M. Berland, *Annu. Rev. Biomed. Eng.* **2000**, *2*, 399.
[44] M. Álvarez, A. Best, S. Pradhan-Kadam, K. Koynov, U. Jonas, M. Kreiter, *Adv. Mater.* **2008**, *20*, 4563.
[45] L. Tu, X. Liu, F. Wu, H. Zhang, *Chem. Soc. Rev.* **2015**, *44*, 1331.
[46] B. Zheng, J. Fan, B. Chen, X. Qin, J. Wang, F. Wang, R. Deng, X. Liu, *Chem. Rev.* **2022**, *122*, 5519.
[47] M. Freitag, N. Möller, A. Rühling, C. A. Strassert, B. J. Ravoo, F. Glorius, *ChemPhotoChem* **2019**, *3*, 24.
[48] N. Bogdan, F. Vetrone, G. A. Ozin, J. A. Capobianco, *Nano Lett.* **2011**, *11*, 835.
[49] W. Li, J. Wang, J. Ren, X. Qu, *J. Am. Chem. Soc.* **2014**, *136*, 2248.
[50] Y. Mi, H. B. Cheng, H. Chu, J. Zhao, M. Yu, Z. Gu, Y. Zhao, L. Li, *Chem. Sci.* **2019**, *10*, 10231.
[51] C. J. Carling, J. C. Boyer, N. R. Branda, *J. Am. Chem. Soc.* **2009**, *131*, 10838.
[52] W. Li, Z. Chen, L. Zhou, Z. Li, J. Ren, X. Qu, *J. Am. Chem. Soc.* **2015**, *137*, 8199.
[53] S. Beyazit, S. Ambrosini, N. Marchyk, E. Palo, V. Kale, T. Soukka, B. Tse Sum Bui, K. Haupt, *Angew. Chem., Int. Ed.* **2014**, *53*, 8919.
[54] J.-C. Boyer, C.-J. Carling, B. D. Gates, N. R. Branda, *J. Am. Chem. Soc.* **2010**, *132*, 15766.
[55] L. Wang, H. Dong, Y. Li, R. Liu, Y.-F. Wang, H. K. Bisoyi, L.-D. Sun, C.-H. Yan, Q. Li, *Adv. Mater.* **2015**, *27*, 2065.
[56] W. Wu, L. Yao, T. Yang, R. Yin, F. Li, Y. Yu, *J. Am. Chem. Soc.* **2011**, *133*, 15810.
[57] L. Wang, A. M. Urbas, Q. Li, *Adv. Mater.* **2020**, *32*, 1801335.
[58] Z. Chen, L. Zhou, W. Bing, Z. Zhang, Z. Li, J. Ren, X. Qu, *J. Am. Chem. Soc.* **2014**, *136*, 7498.
[59] S. Xu, S. Xu, Y. Zhu, W. Xu, P. Zhou, C. Zhou, B. Dong, H. Song, *Nanoscale* **2014**, *6*, 12573.
[60] Y. Fu, G. Alachouzos, N. A. Simeth, M. Di Donato, M. F. Hilbers, W. J. Buma, W. Szymanski, B. L. Feringa, *Chem. Sci.* **2023**, *14*, 7465.
[61] H. Wei, W. Zheng, X. Zhang, H. Suo, B. Chen, Y. Wang, F. Wang, *Adv. Opt. Mater.* **2022**, *11*, 2201716.
[62] B. Shen, S. Cheng, Y. Gu, D. Ni, Y. Gao, Q. Su, W. Feng, F. Li, *Nanoscale* **2017**, *9*, 1964.
[63] Z. Lei, X. Ling, Q. Mei, S. Fu, J. Zhang, Y. Zhang, *Adv. Mater.* **2020**, *32*, 1906225.
[64] Z. Chen, W. Sun, H.-J. Butt, S. Wu, *Chem. – A Eur. J.* **2015**, *21*, 9165.
[65] M. Kaiser, C. Würth, M. Kraft, I. Hyppänen, T. Soukka, U. Resch-Genger, *Nanoscale* **2017**, *9*, 10051.
[66] H. Song, B. Sun, T. Wang, S. Lu, L. Yang, B. Chen, X. Wang, X. Kong, *Solid State Commun.* **2004**, *132*, 409.
[67] C. M. S. Jones, A. Gakamsky, J. Marques-Hueso, *Sci. Technol. Adv. Mater.* **2021**, *22*, 810.
[68] H. S. Yu, X. He, S. L. Li, D. G. Truhlar, *Chem. Sci.* **2016**, *7*, 5032.
[69] J. Zheng, X. Xu, D. G. Truhlar, *Theor. Chem. Acc.* **2011**, *128*, 295.
[70] A. V. Marenich, C. J. Cramer, D. G. Truhlar, *J. Phys. Chem. B* **2009**, *113*, 6378.
[71] G. Alachouzos, A. M. Schulte, A. Mondal, W. Szymanski, B. L. Feringa, *Angew. Chem., Int. Ed.* **2022**, *61*, e202201308.
[72] A. M. Schulte, G. Alachouzos, W. Szymański, B. L. Feringa, *J. Am. Chem. Soc.* **2022**, *144*, 12421.
[73] Z. Yu, W. K. Chan, T. T. Y. Tan, *Small* **2020**, *16*, 1905265.